

Pressurized Gyration: Fundamentals, Advancements, and Future

Yanqi Dai,* Jubair Ahmed, and Mohan Edirisinghe*

As a facile, efficient, and low-cost fiber manufacturing strategy, pressurized gyration/rotation (PG) is attracting tremendous attention. This review provides a comprehensive introduction to the working setups, fundamental principles, processing parameters, and material feed properties of this technology. The characterizations of products prepared by this technology and their wide application fields are summarized. The development potentials and broader application prospects of PG are discussed. PG holds significant promise for the scale-up of ultrafine fiber manufacturing.

1. Introduction

Although the mastery of fiber-forming technologies can be traced back to hundreds of years ago, the enthusiasm for research in this field has never faded.^[1–3] Polymeric fibers at the nano- and micro-scale can have an extremely high surface area-to-volume ratio compared with macroscopic materials, as well as adjustable porosity, suitable mechanical strength, and unique surface effects. These astonishing features make such fibers desirable materials for filtration, textiles, nano-catalysis, optoelectronic components, tissue engineering scaffolds, drug delivery systems, disease diagnosis, etc.^[4–13] Especially since the outbreak of SARS-CoV-2, public health and personal protection have raised more concern, leading to a surge in the demand for fiber-based personal protection equipment.^[14,15] Therefore, there is an increasing urge to find a simple, efficient, low-cost, flexible, and controllable fiber manufacturing method to meet the exponentially surging demand.

Currently, there are diverse strategies for the formation of these fibers, including template synthesis, phase separation, self-assembly, and electrospinning.^[16–20] Although template synthesis, phase separation, and self-assembly have been used to produce ultrafine nanofibers with desirable patterns,^[21–24] they are

not ideal for fiber manufacturing. The fiber-forming processes of these techniques are cumbersome and time-consuming, as well as difficult to form continuous nanofibers. Electrospinning overcomes the limitations of these technologies and can prepare uniform and continuous nanofibers through a simple process.^[1,25] As a result, electrospinning has become one of the most widely used fiber production methods. However, a typical electrospinning setup only forms one fiber from a single needle, which greatly limits its potential for scale-up.

Forcespinning (centrifugal spinning) is a nozzle-free spinning technology driven by centrifugal force, which allows multiple fibers to be drawn from different orifices at the same time.^[26] Forcespinning effectively improves fiber production efficiency. This technology bypasses the high-voltage electric field used in electrospinning, eliminating the consequences of negative incidents. Due to the above advantages, nozzle-free spinning technologies are attracting more attention.

Pressurized gyration (PG), as the name suggests, is a scalable fiber-forming technology that combines high-pressure and rotary jet spinning systems.^[27] PG generates fibers via the combination of centrifugal force and gas blowing, bypassing the high-voltage electric field required in electrospinning. This allows PG to have a wider range of potential materials it can process. In addition, PG achieves a fiber production rate much higher than that of typical single-needle electrospinning by a facile one-pot method. Compared with centrifugal spinning, the introduction of the high-pressure system in PG facilitates the formation and stretching of spinning jets, resulting in higher fiber yield and thinner fibers. Highly controllable processing parameters, easy-to-replace spinnerets, and a wider choice of materials are unique advantages of PG for fiber customization. This paper systematically reviews the fundamental principles, development history, and prospects of producing polymeric fibers by PG, aiming to improve the understanding of this fascinating technology and promote the innovation of fiber-forming technologies in the modern material age.

Y. Dai, J. Ahmed, M. Edirisinghe
 Department of Mechanical Engineering
 University College London
 Torrington Place, London WC1E 7JE, UK
 E-mail: yanqi.dai.19@ucl.ac.uk; m.edirisinghe@ucl.ac.uk

 The ORCID identification number(s) for the author(s) of this article can be found under <https://doi.org/10.1002/mame.202300033>

© 2023 The Authors. Macromolecular Materials and Engineering published by Wiley-VCH GmbH. This is an open access article under the terms of the Creative Commons Attribution License, which permits use, distribution and reproduction in any medium, provided the original work is properly cited.

DOI: 10.1002/mame.202300033

2. Fundamentals of Pressurized Gyration

The PG system mainly consists of three sections: the spinning vessel, the high-pressure gas circuit, and the collector (**Figure 1**). In the typical laboratory PG setup, the spinning vessel is an aluminum perforated cylindrical container (bottom diameter and side height are 60 and 35 mm, respectively). The number of orifices on the vessel wall is about 20, and the diameter of each orifice is 0.5 mm. The spinning vessel is connected by

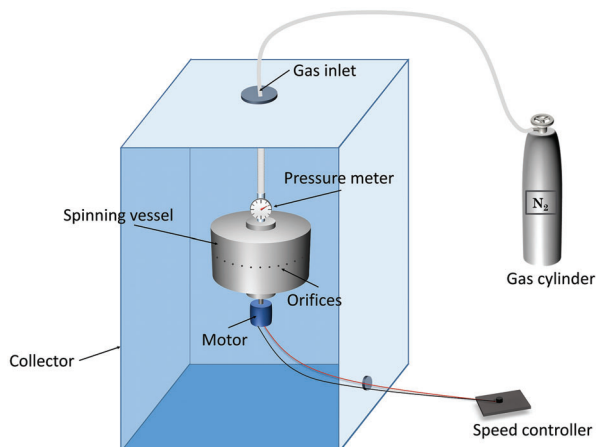


Figure 1. Schematic diagram of the pressurized gyration setup, consisting of a gyro-vessel, an electrical motor, a gas cylinder, and a collecting frame.

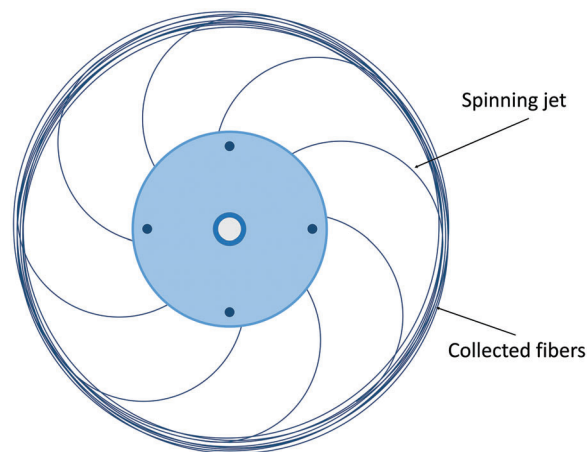


Figure 2. Top view of jet pathway and collected fibers in pressurized gyration.

bearings to an electrical motor, which provides a rotational speed of usually up to 36 000 rpm. The electrical motor is connected to a speed control knob to set the desired speed while spinning. The lid of the spinning vessel is connected to a nitrogen gas cylinder through plastic tubing, which can provide a working pressure of up to 3×10^5 Pa. The collector is placed at a certain distance from the spinning vessel (≈ 100 – 200 mm) to collect dry fibers with the desired morphology.

The fiber formation in PG can be summarized into three main stages, namely jet initiation, jet extension, and solvent evaporation.^[28] Upon starting the spinning process, the polymer fluid is rapidly spread in the spinning vessel under the centrifugal force provided by the motor. The fluid profile has been seen to assume a parabolic shape.^[29] After applying the nitrogen gas flow, the polymer fluid reaches the orifices at approximately the same time, which means that they have an almost equal initial velocity (kinetic energy) and height (potential energy). Subsequently, the polymer fluid starts to overflow from the orifices. The polymer droplets at the orifices form a surface tension gradient along the air-liquid interface under the action of external forces, such as centrifugal force, and pressure differences.^[30] The equation of the destabilizing gravitational force per volume to the stabilizing surface tension force per volume can be used to define the instability between the air-liquid interface, where ρ is the density of the liquid, g is the gravitational acceleration, γ is the liquid-gas surface tension, h and x are the height of the liquid film hanging under the horizontal surface and the direction parallel to the ceiling, respectively.^[30]

$$\rho g \frac{\partial h}{\partial x} = \gamma \frac{\partial^3 h}{\partial x^3} \quad (1)$$

In the PG process, gravitational force in Equation (1) is replaced by destabilizing centrifugal force ($\rho\omega^2 r$) and orifice pressure difference (Δp), where ω and r are the rotational speed and the radius of the vessel, respectively.^[27] Thus, the characteristic length scale of the instability (L_{insta}) can be defined as:

$$L_{\text{insta}} = \left[\frac{h\gamma}{(\rho\omega^2 r) + \Delta p} \right]^{1/3} \quad (2)$$

The polymer droplet expands outward in the direction of decreasing surface tension and forms a ‘finger’ shape (Marangoni effect).^[31] This process is defined as jet initiation. Due to the high viscosity of the spinning fluid, the ejected fluid does not break into individual droplets but forms continuous jets. During the jet extension stage, the polymer jets leaving the orifice continue to move outward and stretch under the action of inertia and pressure difference. At this stage, the polymer jets are also subjected to centrifugal force, forming curved jets around the circumference of the spinning vessel (Figure 2). The air resistance at the air-liquid interface promotes the elongation and subsequent thinning of the jets. During the jet movement, the solvent gradually evaporates, resulting in the further thinning of spinning jets. The dry fibers are eventually deposited on the collector. The fibers produced by this process generally have higher alignment than electrospun fibers that undergo whipping motions.

2.1. System Parameters

2.1.1. Rotational Speed

The electrical motor is one of the significant components of the PG device. After energization, the motor drives the spinning vessel to rotate at a speed of usually up to 36 000 rpm. The polymer fluid loaded in the vessel is subjected to centrifugal force (F_{centri}). According to Newton’s second law:

$$F_{\text{centri}} = m\omega^2 r \quad (3)$$

where m is the mass of the spinning fluid, ω and r are the rotational speed and the radius of the vessel, respectively. From Equation (3), it can be seen that the centrifugal force of the spinning fluid increases as the rotational speed increases. Only when the centrifugal force is sufficient to overcome the surface tension of the spinning fluid, spinning jets can be formed and ejected from the orifices. The minimum rotational speed that provides this centrifugal force is known as the critical rotational speed. When the rotational speed is lower than the critical value, spinning jets cannot be formed. In addition, the solvent may separate from the polymer and solvent loss occurs in this case.^[32]

After the polymer fluid is ejected from the vessel, these jets are simultaneously subjected to centrifugal force and air resistance (F_{air}).

$$F_{\text{air}} = \frac{1}{2} \pi C \rho A \omega^2 D^2 \quad (4)$$

where C is the numerical drag coefficient, ρ is the air density, A is the cross-sectional area of the spinning jet, ω is the rotational speed of the jet, and D is the diameter of the jet pathway.^[33] According to Equations (3) and (4), both the centrifugal force and air resistance of the spinning jets increase with the increase of the rotational speed, which is beneficial to the stretching of the jets to form finer long fibers. Conversely, at relatively low rotational speeds, PG usually produces thicker and shorter fibers or droplets due to insufficient stretching.

2.1.2. Working Pressure

The most prominent feature of PG is the incorporation of a high-pressure system with rotary jet spinning. Working pressure is an important influencing factor of fiber diameter. Compared to rotary jet spinning without pressure, the pressure provided by PG increases the acceleration of the spinning flow. The spinning flow is then ejected from the orifices at a larger initial velocity. The higher the pressure, the shorter the time required for jet formation. In addition, high working pressure facilitates the stretching of the spinning jets into finer fibers. This is related to the fact that the pressure increases the kinetic energy of the spinning jets, which helps with the additional elongation during the stretching stage. According to the microscopic jet flow model reported by Gañán-Calvo et al., the liquid jet diameter (d_j):

$$d_j \cong \left(\frac{8\rho}{\pi^2 \Delta p} \right)^{1/4} Q^{1/2} \quad (5)$$

where ρ is the density of the liquid, Δp is the pressure difference and Q is the flow rate.^[34] Equation (5) suggests the inversely proportional relationship between jet diameter and pressure difference, which is consistent with experimental results.^[27]

The working pressure also affects the morphology and alignment of fibers. A higher working pressure results in greater kinetic energy of the spinning jets but also increases their kinematic instability, leading to bead formation and lower fiber alignment.^[35] A balance between the gas flow rate and the liquid flow rate is conducive to obtaining smooth bead-free fibers.^[36] The solvent evaporates from the spinning jets, causing a local temperature drop due to the enthalpy of vaporization.^[37] The temperature drop may lead to the condensation of water vapor on the fiber surface. When these water droplets evaporate, their imprints remain to form the porous architecture on the fiber surface. Higher working pressures will cause faster solvent evaporation, promoting the formation of additional pores.^[32]

2.1.3. Vessel Design

The spinning vessel, which operates at ambient temperature, is also an important component of the PG setup. During the spinning process, the loaded spinning fluid travels the vessel walls

and extrudes from the liquid channels while overcoming its own surface tension. Therefore, the material properties, dimensions, and geometry of the vessel have a significant impact on fiber morphology. In the reported studies, the PG vessel is a metal or plastic cylinder (60 mm diameter \times 35 mm height) consisting of a perforated reservoir and an adapted lid.^[27,29] Different friction factors exist between the spinning fluid and the vessels made of different materials, which affect the flow behavior and the formation of spinning jets. In addition, different vessel materials have different densities and melting points, these effect the vessel weight and processing temperature. Generally, metals with a low density, such as aluminum, are favored. An optically transparent polymeric vessel, on the other hand, facilitates the study of fluid behavior inside the vessel.^[29]

Fiber morphology is also affected by vessel dimension. From Equations (1) and (2), it can also be seen that the centrifugal force and air resistance subjected to the spinning fluid increase with increasing vessel radius. Therefore, at a constant rotational speed, increasing the vessel radius facilitates the formation and stretching of the spinning jets, in turn reducing the fiber diameter.

In a typical PG setup, multiple orifices (up to 24) with a diameter of 0.5 mm are distributed along the perimeter of the vessel wall at equal intervals, allowing the formation of multiple spinning jets at the same time.^[27,32,38,39] Thus PG is considered as a very promising manufacturing technology for fiber mass production. When the orifices are replaced with external nozzles, PG can be used to produce polymeric fibers with uniform morphology and well-defined alignment.^[35] This is because directing the spinning fluid through nozzles is beneficial in improving the stability of the flow state. In addition, vessels with multi-layer reservoirs have been used for the preparation of core-sheath fibers.^[40,41] The inner and outer reservoirs are loaded with different polymer solutions to form the core and the sheath structures of the multi-layer fibers, respectively.

2.1.4. Collection

To collect the solidified fibers, collectors made of metals or plastics are positioned at a specific distance from the spinning vessel. In addition to the collecting frame (Figure 1), collecting meshes (Figure 3A) and surrounding collecting rods (Figure 3B) can also be used with PG. Compared to collecting frames, collecting rods and collecting meshes are more favorable for solvent evaporation due to exposure of the convective air. In addition, these collectors improve fiber alignment. The effect of collection distance on fiber morphology is also significant. When the collection distance is too little, the jet stretching is insufficient, forming thicker and shorter fibers. Additionally, a very short collection distance may result in insufficient solvent evaporation to form beaded fibers or the deposition of wet (non-dried) jets on the collector which can be seen as deposited liquid.^[42] Increasing the collection distance facilitates the elongation of spinning jets and reduces the fiber diameter. However, a collection distance which is too far, will cause jet rupture and fewer fibers will be collected. The optimal collection distance for the PG system varies with solution properties, solvent volatility, flexibility and ductility of the polymer, ambient temperature, relative humidity, etc.

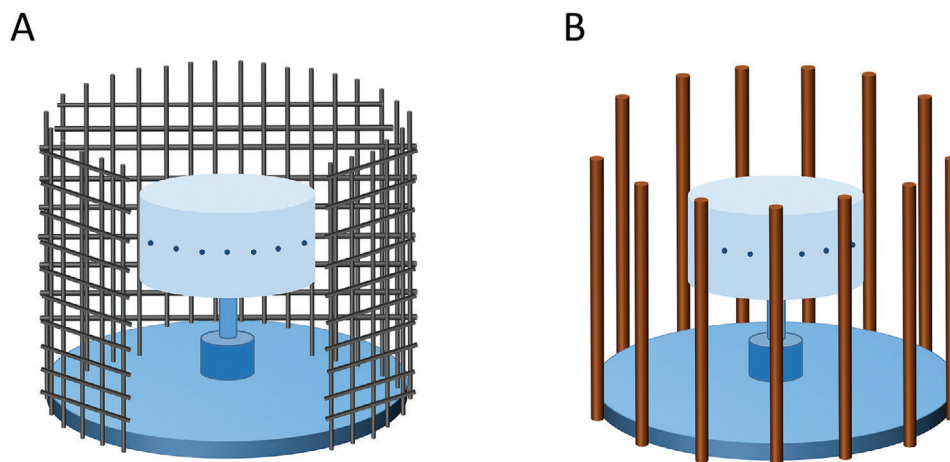


Figure 3. Different designs of collectors: A) collecting meshes and B) collecting rods.

2.2. Spinning Fluid Properties

The spinnability of spinning fluid (polymer solution/polymer melt) and the morphology and structure of fibers in PG are significantly affected by the inherent properties of the spinning fluid, such as molecular structure, molecular weight, crystallinity, solution concentration, viscosity, surface tension, and solvent volatility. Among them, the influence of surface tension and viscosity plays the most dominant role in the PG system, while other fluid properties affect the spinning process by changing these two main properties.

Not all polymer fluids can form fibers through the PG process. The ability of the spinning fluid to be stretched into fine jets is referred to as its spinnability, which is dependent on the viscoelasticity of the spinning fluid.^[43] In general, the viscosity of a polymer solution increases with the increase of its concentration. Only when the solution concentration meets the critical value, which is determined by polymer molecular weight and solvent type, can the corresponding viscoelasticity provide sufficient chain entanglement to form spinning jets. Polymer solutions with concentrations below the critical value will typically only form droplets due to insufficient chain entanglement. However, the increase in solution viscosity imposes greater resistance to the centrifugal force and dynamic fluid blowing, as well as to inhibit solvent evaporation.^[27] Thus for spinnable polymer solutions, the fiber diameter increases with the increase of solution concentration. When the solution viscosity is too high, the centrifugal force cannot overcome the surface tension. Spinning jets can therefore not be formed in this scenario. The presence of beads is also affected by solution concentration. With the increase in concentration, the product of PG under the same working parameters gradually transitions from bead-on-string fibers to smooth fibers without beads.^[44] For polymer melts, the viscosity is usually adjusted by changing the polymer molecular weight and processing temperature.

As a consequence, the morphology of the final products in PG is influenced by a combination of factors that compete with one another, including surface tension, viscosity, rotation speed, air velocity, etc. Building on a simple mathematical model for rotary jet spinning from Mellado et al.,^[28] the relationship between the

fiber diameter and the various processing parameters in PG can be established.^[32]

$$r_j = \frac{r_0 U^{3/2} \nu^{1/2}}{R_c^{3/2} \omega V_a} \quad (6)$$

where r_0 and r_j are the radius of the initial jet and the final jet, respectively. $\nu = \frac{\mu}{\rho}$ is the kinematic viscosity, R_c is the radius of the collector, U is the initial velocity and ω is the angular velocity. V_a is the air velocity. **Table 1** summarizes the effects of different parameters on the produced fibers.

3. Sister Technologies

3.1. Pressure-Coupled Infusion Gyration

As a fiber mass production method, PG has achieved a production efficiency orders of magnitude higher than that of electrospinning, while there are still limitations.^[27] The typical PG cannot support the continuous spinning process. To advance the industrialization of the PG technique, Hong et al. introduced a syringe pump into PG devices, named pressure-coupled infusion gyration (PCIG).^[45] Polymer solutions can be continuously fed into the spinning vessel at a specific flow rate. Fiber diameter and distribution as well as fiber morphology can be adjusted by infusion flow rate. In addition, the increasing flow rate effectively increases fiber yield. Compared to typical PG, PCIG produces fibers with smaller diameters under the same solution properties and system parameters. The effect of interaction parameters (solution concentration, working pressure, rotational speed, and infusion flow rate) on fiber diameter in PCIG has been established by effective and reliable mathematical models, which is in high agreement with experimental results.^[47,48] (**Figure 4**)

3.2. Pressurized Melt Gyration

To avoid potential toxicity and environmental issues caused by organic solvents, Xu et al. proposed pressurized melt gyration

Table 1. The effects of system parameters and spinning fluid properties.

		Fiber Diameter	Bead	Others
System Parameters	Rotational Speed ↑	↓	↓	Fiber Length ↑ Bead Size ↓ Uniformity ↓
	Working Pressure ↑	↓	↑	Fiber Length ↑ Bead Size ↑ Uniformity ↓ Yield ↑
	Collection Distance ↑	↓		Fiber Length ↑ Uniformity ↓
	Infusion Flow Rate (PCIG) ↑	↑	↑	Yield ↑
	Melting Temperature (PMG) ↑	↓		Surface Roughness ↑
Spinning Fluid Properties	Molecular Weight ↑	↑	↓	Bead Size ↑ Fiber Length ↓
	Concentration ↑	↑	↓	Bead Size ↑ Fiber Length ↓
	Solvent Volatility ↑	↓		Pore Size ↑
Others	Temperature ↑			Solvent Evaporation ↑
	Humidity ↑			Pores ↑

*↑ and ↓ denote increase and decrease respectively. PCIG and PMG denote pressure-coupled infusion gyration^[45] and pressurized melt gyration,^[46] respectively. It should be noted that these are the most common overall outcomes. Exceptions may exist for some polymer systems used.

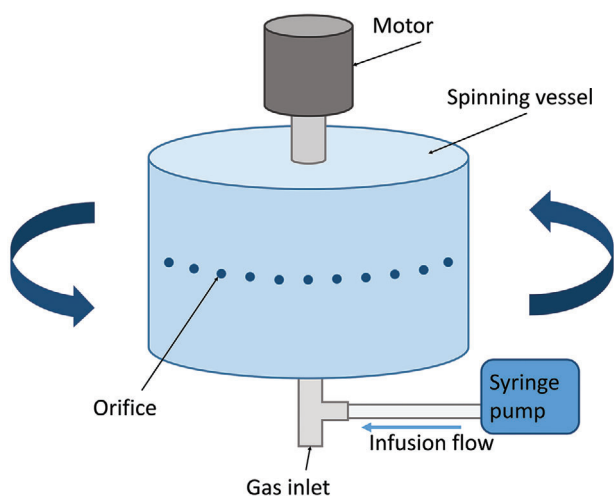


Figure 4. Schematic diagram of pressure-coupled infusion gyration.

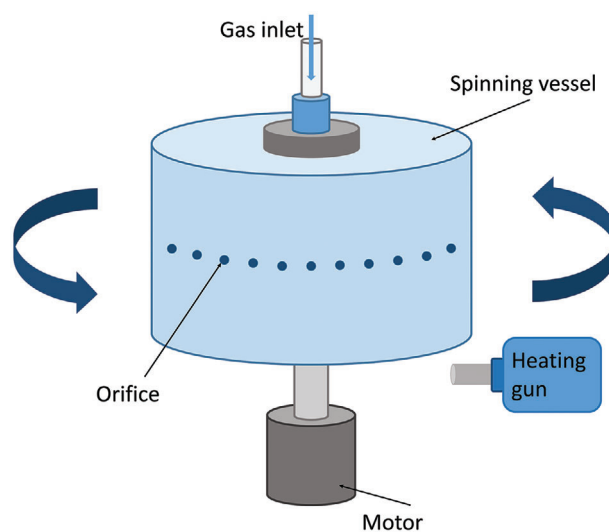


Figure 5. Schematic diagram of pressurized melt gyration.

(PMG) by combining melt spinning and pressurized gyration.^[46] The heating gun fixed on the PMG setup increases the temperature of the spinning vessel (up to 600 °C), resulting in a polymer melt. An in situ thermocouple is used to monitor and control the system temperature. A higher temperature reduces the viscosity of the polymer melt, which facilitates the formation of finer fibers. The Ag nanoparticle-loaded PCL scaffolds prepared by PMG show excellent antibacterial properties and cell viability.^[46] (Figure 5)

3.3. Core-Sheath Pressurized Gyration

Biphasic fibers are produced by the multi-layer design of the spinning vessel in core-sheath pressurized gyration (core-sheath PG).^[40,41] As shown in Figure 6A, the spinning vessel of core-sheath PG has a dual-layered reservoir. The inner and outer reservoirs are used to load different polymer solutions to form the core structure and sheath structure of fibers, respectively. To form a uniformly encapsulated core-sheath structure, the essential condition is the flow synchronization between the inner and outer polymer solutions. Therefore, before the core-sheath PG process,

the flow rate and production rate of the spinning solution loaded in the outer reservoir are required to be tested. Then the inner solution is manipulated to match a synchronous flow. In core-sheath PG, the liquid volume ratio of core-solution and sheath-solution is an important factor. A portable core-sheath PG device designed by Alenezi et al. has been demonstrated to achieve continuous large-scale production of core-sheath nanofibers in a facile step.^[49] The solid core and sheath of core-sheath fibers are formed from different polymers (Figure 6B), providing different physical and chemical properties.^[50] Core-sheath polymer fibers produced by core-sheath PG are fascinating candidates for biomedical materials that are used in tissue engineering scaffolds, drug release, and wound healing bandages.^[51,52]

3.4. Nozzle-Pressurized Gyration

Nozzle-pressurized gyration (nozzle-PG), as the name suggests, replaces the small orifices on the PG spinning vessel with external nozzles.^[35] Nozzle-PG is the novel sister technology of the

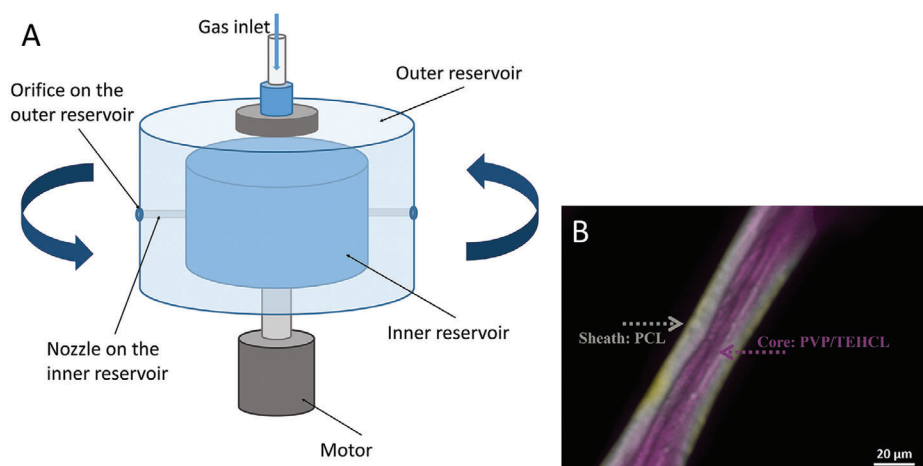


Figure 6. A) Core-sheath pressurized gyration device and B) confocal microscopy image of PVP/PCL core-sheath fiber. Reproduced with permission.^[52] Copyright 2022, Elsevier.

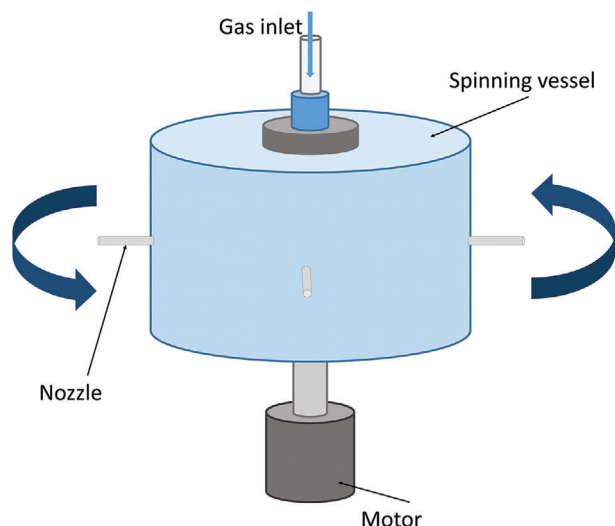


Figure 7. Schematic diagram of nozzle-pressurized gyration.

PG technique. By directing the spinning solution through nozzles, this significantly improves its flow stability, thereby improving the uniformity and alignment of the produced fibers. In addition, the fibers prepared by nozzle-PG have smaller fiber diameters and narrower diameter distributions compared to those of PG under the same working parameters. Although spinning technologies with nozzles are often associated with nozzle clogging, the high-velocity nitrogen flow in nozzle-PG helps flush the nozzles, thereby alleviating the clogging issues. Fibers produced by nozzle-PG are promising for specific applications that are sensitive to fiber diameters and arrangements, such as precision biosensors and tissue engineering. (Figure 7)

The design and quantity of nozzles are the critical parameters in nozzle PG as it significantly affects the airflow field distribution and flow behavior, which can influence the morphology and yield of the final products. Generally, nozzles with a very small diameter can produce fine fibers. However, they will lead to nozzle clogging and lower throughput. Whereas, increasing the nozzle

diameter will increase the fiber diameter accordingly. Throughput can also be increased by increasing the number of nozzles so as to achieve higher fiber yields. In terms of nozzle length, increasing the nozzle length may make the fluid more difficult to eject from the nozzles. Further studies need to be performed to optimize the nozzle design to achieve the maximum possible throughput and desired fiber morphology.

4. Materials for Pressurized Gyration

Thus far, there have seen a wide variety of materials processed by PG and its sister technologies. The applications of these fibrous products span a wide range of areas, especially in filtration and healthcare. Compared with electrospinning, PG averts the influence of high voltage on sensitive materials, as well as providing more options in materials and solvents due to its controllable environmental conditions. In addition to common synthetic polymeric fibers (polyethylene oxide, polycaprolactone, polyvinylpyrrolidone, poly(methyl methacrylate), polyacrylonitrile, polylactic acid, etc.),^[27,35,38,53–56] biopolymer fibers were also spun using PG, including silk fibroin, polyhydroxyalkanoates, starch, etc.^[57–60] These fibers have broad prospects in biomedical applications due to their inherent biocompatibility and environmental friendliness. Carbon nanofibers with polyacrylonitrile as the precursor can be easily produced by PG.^[55] Carbon nanofibers have attracted increasing attention as supercapacitors, fuel cells, battery electrodes, etc. due to their unique electrochemical properties.^[61,62] Moreover, ceramic fibers, such as polymethyl-silsesquioxane (MK resin), polymethylphenyl-silsesquioxane (H44 resin), also have been successfully made by PG technology.^[63] The products of PG are diverse in terms of their structures. Besides uniform solid fibers, PG has been used to produce beaded fibers, core-sheath fibers, and microbubbles instead of one-dimensional materials.^[40,44,64,65] Microbubbles are a promising material in diagnosis, therapeutic applications, targeted drug delivery, etc.^[66–69] These successful instances undoubtedly validate the practicability and extensibility of the PG technology in the preparation of micro/nano-materials. **Table 2**

Table 2. Polymeric materials processed by pressurized gyration, detailed information of final products and their potential applications.

Polymer	Molecular Weight	Solvent	Concentration	Agent	Product Type	Average Fiber Diameter	Application	Technique	Ref.
Polycaprolactone (PCL)	$M_w = 8 \times 10^4 \text{ g mol}^{-1}$	Acetone	5%–30% (w/v)		Beads, beaded fibers, fibers	Bead: 145–660 μm fiber: 3–23 μm	Drug delivery	PG	[44]
		Chloroform	15% (w/v)	Nano-clay, (2–5 wt.%)	Microfiber scaffolds	1.1–3.9 μm	Bone tissue regeneration	PG, Nozzle-PG	[35, 70]
			10–12 wt.%	Tetracycline hydrochloride (TEHCL, 2 wt.%)	Porous fibers	1.7–5 μm	Drug release (antimicrobial and anti-inflammatory), wound dressing	PG	[52, 71]
	$M_n \approx 8 \times 10^4$	Chloroform	15% (w/v)	Cinnamon powder (250–500 mg mL ⁻¹)	Fiber meshes	1.7–6 μm	Antimicrobial fibers, wound healing bandages	PG	[72, 73]
Polyethylene oxide (PEO)	$M_w = 2 \times 10^5 \text{ g mol}^{-1}$	Water	Molten liquid (95–200 °C)	Ag nanoparticle (0.01% (v/v))	Microfiber scaffolds	14–38 μm	Antibacterial fibers, muscular tissue engineering	PMG	[46]
			5–21 wt.%	DsRed-AuBP2-engineered protein, Au nanoparticle	Nanofibers	50–1085 nm	Aligned nanofibers	PG, PCIG, Nozzle-PG, Infusion Gyration	[27, 29, 35, 48, 58, 74]
Poly(methyl methacrylate) (PMMA)	$M_w = 1.2 \times 10^5 \text{ g mol}^{-1}$	N,N-dimethyl-formamide (DMF)	30% (w/v)		Nanofibers	$\approx 290 \text{ nm}$		PG	[75]
		Chloroform	20% (w/v)	Hydroxyapatite (HA, 10 wt.%)	Porous nanofibers	$\approx 800 \text{ nm}$	Targeted therapy (leukemia)	PG	[76]
		Chloroform, acetone, DMF, ethyl acetate, dichloromethane (DCM)	20 wt.%	Graphene nanoplatelet (0–8 wt.%), graphene oxide nanosheet (0–8 wt.%), tungsten oxide nanoparticle (0–8 wt.%), W-Ag-Cu nanoparticle (0–0.5 wt.%)	Microfibers with smooth/porous surfaces	1–20 μm	Antibacterial and antiviral fibers	PG	[53, 77–81]
Polyvinyl-pyrrolidone (PVP)	$M_w = 2.8 \times 10^4 - 1.5 \times 10^6 \text{ g mol}^{-1}$	Phosphate-buffered saline (PBS), ethanol	10%–30% (w/v)		Nanofibers	462–971 nm	Pharmaceutical sciences, binders, drug delivery	PG	[38, 82]
	$M_w = 1 \times 10^5 - 1.5 \times 10^5 \text{ g mol}^{-1}$	Ethanol	10% (w/v)	Ibuprofen (10%–50% (w/v))	Microfibers	1.2–5.4 μm	Oral administration, drug delivery	PG	[82]
	$M_w = 1.3 \times 10^6 \text{ g mol}^{-1}$	Ethanol	10%–15% (w/v)	Amphotericin B (5 wt.%), itraconazole (2.5 wt.%)	Uniform fibers with high alignment	1.3–3.5 μm	Drug delivery	PG, Nozzle-PG, Core-sheath PG	[35, 52, 81]

(Continued)

Table 2. (Continued).

Polymer	Molecular Weight	Solvent	Concentration	Agent	Product Type	Average Fiber Diameter	Application	Technique	Ref.
Poly-acrylonitrile (PAN)	$M_w = 1.5 \times 10^5 \text{ g mol}^{-1}$	A mixture of ethanol and methanol (4:1 v/v) N, N-dimethyl-formamide (DMF)	10%–20% (w/v) 4%–15% (w/v)	Pioglitazone hydrochloride (PHR, 12 mg mL ⁻¹) Graphene oxide (3–10 wt.%, graphene nanoplatelets (GNPs, 0–8 wt.%), Carbon nanotubes (CNTs, 0–0.5 wt.%)	Smooth fibers Pore-free nanofibers Carbon fiber	0.6–3.2 μm 200–520 nm 0.7–20 μm	Biodegradable drug release system (diabetic wounds) Conductive fiber, energy storage devices	PG PG PG	[83] [75, 84] [54, 85]
Poly(vinyl alcohol) (PVA)	$M_w = 1.46 \times 10^5 - 1.86 \times 10^5 \text{ g mol}^{-1}$	Water	10 wt.% 10% (w/v)	Cold nanoparticle, lysozyme (4% (w/v)),	Carbon nanofiber Microbubbles	400–800 nm 10–250 μm	Energy storage device, supercapacitors Antibacterial fibers, biosensors, intracellular probes, ultrasound contrast agents, drug delivery	PG PG	[55] [64, 65]
Poly(lactic acid) (PLA)	$M_w = 1.1 \times 10^5 \text{ g mol}^{-1}$	Chloroform	8%–15% (w/v)	Progesterone (10 wt.%)	Drug-loaded fibrous patches	6.8–26 μm	Sustained drug release system (preterm birth)	PG	[56, 71]
Polyvinylidene fluoride (PVDF)	$M_w = 2.75 \times 10^5 \text{ g mol}^{-1}$	A mixture of DMF and acetone	15%–25% (w/v)		Beaded fibers	1.6–26 μm	Face masks	PG	[81, 86]
Polyethylene (terephthalate) (PET)	$M_w = 1 \times 10^5 \text{ g mol}^{-1}$	Trifluoro acetic acid, trichloro acetic acid	20 wt.%		Nanofibers	290–714 nm		PG	[87]
Nylon 6.6	$M_w = 3 \times 10^4 \text{ g mol}^{-1}$	Formic acid	5–20 wt.%	Ag nanoparticle (1–4 wt.%)	Nanofibers	50–500 nm	Antibacterial fibers	PG	[88]
Thermoplastic polyurethane (TPU)		N, N-dimethyl-formamide (DMF)	15–25 wt.%	Graphene nanoplatelet (5 wt.%)	Microfibers	1–13 μm	Fuel cells, electronic packaging	PG	[89]
Poly-acrylamide (PAM)		(Hydrogel)		Montmorillonite (0.89 wt.%, chitosan (0.16 wt.%)	Composite hydrogel fibers	≈ 5.5 μm		PG	[90]
Poly(N-isopropylacrylamide) (PNIPAm)	$M_w = 3 \times 10^5 \text{ g mol}^{-1}$	A mixture of chloroform and ethanol (2:1, v/v)	20% (w/v)		Pore-free fibers	≈ 6.3 μm		PG	[81]
Cyclodextrin		Water	180%–220% (w/v)		Pore-free fibers	5.5–6.5 μm		PG	[91]
Polyhydroxyalkanoates (PHAs)	$M_w > 4 \times 10^5 \text{ g mol}^{-1}$	Chloroform	7.4 wt.%	Hydroxyapatite (HA) nanopowder (10 wt.%)	Porous fibers with high alignment	2.5–9.1 μm	Hard (bone) and soft (nerve and cardiovascular) tissue engineering	PG	[59]

(Continued)

Table 2. (Continued).

Polymer	Molecular Weight	Solvent	Concentration	Agent	Product Type	Average Fiber Diameter	Application	Technique	Ref.
Silk fibroin (SF)		1,1,1,3,3,3-hexafluoro-2-propanol (HFIP)	8–12% (w/v)		Pore-free fibers	0.8–30 μm	Tissue engineering, filtration	PG	[57, 58]
PCL/PVA	$M_w = 8 \times 10^4 / 5 \times 10^4 \text{ g mol}^{-1}$	Chloroform/water	10 wt.% / 10wt%	Hydroxyapatite (HA) nanoparticle (1–10 wt.%)	Core-sheath fibers	3–4 μm	Bone tissue engineering	Core-sheath PG	[51]
PCL/bacterial cellulose (BC)	$M_w(\text{PCL}) = 8 \times 10^4 \text{ mol}^{-1}$	Chloroform	12 wt.% ($w_{\text{PCL/BC}} = 9:1-1:9$)		Composite fibers	5–9 μm		PG	[71]
PEO/PMMA	$M_w = 2 \times 10^5 / 1.2 \times 10^5 \text{ mol}^{-1}$	Water/chloroform	15 wt.% / 15wt%	Ag-Cu-W composite nanoparticle	Core-sheath fibers	Core: 6–9 μm sheath: 21–32 μm	Filtration, tissue engineering	Core-sheath PG	[40]
PEO/PVP	$M_w = 2 \times 10^5 / 5 \times 10^6 \text{ g mol}^{-1}$	Water/water	15 wt.% / 15wt%		Core-sheath nanofibers	331–998 nm		Core-sheath PG	[41]
PEO/PCL	$M_w = 6 \times 10^5 / 8 \times 10^4 \text{ g mol}^{-1}$	Water/a mixture of chloroform and methanol (3:1, v/v)	10 wt.% / 20 wt.%		Core-sheath nanofibers	≈ 740 nm		Core-sheath PG	[49]
PEO/PLA	$M_w = 6 \times 10^5 / 1.1 \times 10^5 \text{ g mol}^{-1}$	Water/a mixture of chloroform and methanol (3:1, v/v)	10 wt.% / 20 wt.%		Core-sheath nanofibers	≈ 529 nm		Core-sheath PG	[49]
PEO/sodium carboxy-methyl-cellulose (CMC)	$M_w = 2 \times 10^5 / 2.5 \times 10^5 \text{ g mol}^{-1}$	Water/a mixture of ethanol and water	12.5–15 wt.% / 0–2.5 wt.%	Progesterone (0–5 wt.%)	Composite nanofibers	161–550 nm	Drug delivery (vaginal therapies)	PG	[92–94]
PEO/sodium alginate (SA)	$M_w = 2 \times 10^5 \text{ g/mol}$ /medium viscosity	Water	11 wt.% / 1 wt.%		Composite nanofibers	≈ 170 nm	Drug delivery (vaginal therapies)	PG	[94]
PEO/poly-acrylic acid (PAA)	$M_w = 2 \times 10^5 / 4.5 \times 10^5 \text{ g mol}^{-1}$	Water	11 wt.% / 1 wt.%		Composite nanofibers	≈ 215 nm	Drug delivery (vaginal therapies)	PG	[94]
PEO/starch	$M_w = 2 \times 10^5 / 1 \times 10^5 \text{ g mol}^{-1}$	a mixture of water and DMSO (1:1, w/w)	7.5–13.5 wt.% / 1.5–7.5 wt.%		composite nanofibers	163–285 nm		PG	[60]
PMMA/PAN	$M_w = 1.2 \times 10^5 / 1.5 \times 10^5 \text{ g mol}^{-1}$	N, N-dimethyl-formamide (DMF)	10 wt.% / 10 wt.%		Nanofibers	≈ 580 nm		PG	[75]
PMMA/bacterial cellulose (BC)	$M_w(\text{PMMA}) = 1.2 \times 10^5 \text{ g mol}^{-1}$	DMF:THF (1:1, w/w)	20–50 wt.% / 5–10 wt.%	Cu-Ag-Zn, CuO, Cu-Ag-WC nanoparticle (0.05–1 wt.%)	Composite fibers	2–36 μm	Wound dressing	PG	[95, 96]
PMMA/poly(L-lactide) (PLLA)	$M_w = 1.2 \times 10^5 \text{ g mol}^{-1}$ / $M_n = 2500$	Chloroform	10 wt.% / 10 wt.%	A mixture of hydroxyapatite and protein	Composite fibers	≈ 17 μm	Shape memory fibers (bone tissue engineering)	PG	[97]

(Continued)

Table 2. (Continued).

Polymer	Molecular Weight	Solvent	Concentration	Agent	Product Type	Average Fiber Diameter	Application	Technique	Ref.
PVP/PCL	$M_w = 1.3 \times 10^6$ $/8 \times 10^4 \text{ g mol}^{-1}$	A mixture of chloroform and methanol (4:1, v/v)	12% (w/v) (W _{PVP} /PCL = 6/4, 7/3, 8/2)	Glibenclamide (GB, 4 mg mL ⁻¹), pioglitazone (PHR, 12 mg mL ⁻¹)	Composite nanofibers	677–900 nm	Biodegradable drug release system (diabetic wounds), wound healing	PG	[83, 98]
PAN/cellulose acetate (CA)	$M_w = 1.5 \times 10^5$ $/3 \times 10^4 \text{ g mol}^{-1}$	A mixture of acetone and DMF (2:1)	10 wt. %	Tetracycline hydrochloride (TEHCL, 2 wt. %)	Core-sheath fibers	4.1–5 μm	Sustained drug release system (antimicrobial and anti-inflammatory), wound healing	Core-sheath PG	[52]
PVA/PCL	$M_w = 8.9 \times 10^4$ – 9.8×10^4 $/8 \times 10^4 \text{ g mol}^{-1}$	Water/a mixture of chloroform and methanol (3:1, v/v)	20 wt. %/20 wt. %	Vanillin (Kosher)	Porous composite fibers	0.5–2 μm	Drug release system	PG	[84]
PVA/PLA	$M_w = 8.9 \times 10^4$ – 9.8×10^4 $/1.1 \times 10^5 \text{ g mol}^{-1}$	Water/a mixture of chloroform and methanol (3:1, v/v)	20 wt. %/20 wt. %		Core-sheath nanofibers	≈ 743 nm		Core-sheath PG	[49]
PLA/PCL	$M_w = 1.1 \times 10^5$ $/8 \times 10^4 \text{ g mol}^{-1}$	Chloroform	12 wt. % (W _{PLA} /PCL = 9:1–1:9)		Composite fibers	5–19 μm		PG	[71]
PLA/bacterial cellulose (BC)	M_w (PLA) = 1.1×10^5 10^5 g mol^{-1}	Water/a mixture of chloroform and methanol (3:1, v/v)	20 wt. %/20 wt. %		Core-sheath nanofibers	≈ 875 nm		Core-sheath PG	[49]
PLA/PCL/bacterial cellulose (BC)	$M_w = 1.1 \times 10^5$ $/8 \times 10^4 \text{ g mol}^{-1}$	Chloroform	12 wt. % (W _{PLA} /PCL/BC = 7:3:3)		Composite fibers	6–19 μm		PG	[71]
Poly(glycerol sebacate) (PGS)/PVA	M_w (PVA) = 3×10^4 – 7×10^4 mol^{-1}	1, 1, 1, 3, 3, 3-hexafluoropropanol (HFIP)	10%–15% (w/v) (W _{PGS} /PVA = 55:45)		Composite fibers	≈ 16 μm	Tissue engineering	PG	[39]
Silk fibroin (SF)/PEO	30% de-gummed/ $M_w = 2 \times 10^5$ g mol^{-1}	Water	40–45 wt. %/ 1.5–3 wt. %		Composite nanofibers	0.7–2.1 μm	Tissue engineering	PG	[58]
Polymethylsilsesquioxane/PVP	$M_w = 9100$ $/1.3 \times 10^6 \text{ g mol}^{-1}$	A mixture of chloroform and DMF (5:3, w/w)	25 wt. %/ 25 wt. %		Ceramic fibers	10–50 μm		PG	[63]
Polymethylphenylsilsesquioxane/PVP	$M_w = 2100$ $/1.3 \times 10^6 \text{ g mol}^{-1}$	A mixture of chloroform and DMF (5:3, w/w)	20.7 wt. %/ 20.7 wt. %	Graphene (3%)	Ceramic fibers	1–8 μm		PG	[63]
Phenolic resin/PVP		N, N-dimethylformamide (DMF)	10–25 wt. %/ 10 wt. %	Graphene nanoplatelet (5 wt. %)	Composite fibers	2–8.5 μm	Fuel cells, electronic packaging	PG	[89]

summarizes the polymers processed using PG and its sister technologies.

5. Applications

In terms of fiber morphology and properties, PG fibers are highly similar to electrospun fibers, indicating that these fibrous products can be theoretically used in similar application areas. Although in this review we highlight biomedical applications such as tissue engineering, drug delivery, wound healing, targeted therapy, etc. PG fibers also have encouraging prospects for filtration, energy storage, catalysis, sensors, electronics, and optical components.^[99,100]

5.1. Biomedical Applications

5.1.1. Tissue Engineering

Polymer fibers play significant roles in tissue engineering as scaffolds supporting cell seeding and tissue growth, as well as carriers of bioactive factors.^[101–103] PG polymer scaffolds serve as a temporary extracellular matrix (ECM) in tissue engineering. The desired 3D structures of these polymer scaffolds provide specific mechanical and biological properties to modulate cellular behavior.^[104] The aligned orientation of fibers induces the polarization and migration of cells along the fiber direction, accelerating wound closure.^[105,106] Seeding cells on PG fiber scaffolds, which typically have a highly aligned orientation, can promote cellular activities. This is due to the regular or defined architecture of the ECM found in the human body.^[107] In addition, the surface topography of PG fibers is determined by solvent type and environmental conditions, which is tunable to form desired pore size and porosity for cell infiltration.^[108,109] PG fiber scaffolds have been reported to be promising material candidates for tissue engineering. For example, the non-woven PCL scaffold fabricated by PMG technology by Xu et al. showed remarkable attachment, growth, and proliferation results for myoblasts.^[46] The fiber surface roughness and porosity of these scaffolds can be tuned by melting temperature to promote muscular tissue regeneration. The PGS/PVA blended fiber scaffold spun by PG possessed unique biocompatibility and non-toxicity. The dermal fibroblasts that adhered to these scaffolds showed superior cell viability, making it a promising material for soft tissue engineering.^[39] Kundu et al. incorporated composite nano-clay and hydroxyapatite into PCL fibers by PG.^[70] The fabricated fibrous scaffolds had good cell viability and promoted osteogenic differentiation, calcium deposition, and collagen formation. Their results also showed that the osteogenic differentiation of mesenchymal stem cells (MSCs) was enhanced with the addition of PCL fibers. The PHA fibers spun by PG not only enhanced bone regeneration but also showed significant application potential in soft tissue engineering such as in nerve and cardiovascular.^[59] A unique advantage of PHA scaffolds in tissue engineering is that additional growth factors are not required. Heseltine et al. achieved the efficient production of aqueous-based silk fibroin using PG.^[58] Osteocytes exhibited significant cellular activity and proliferation on these aligned silk fibroin fibers. The core-sheath fibers manufactured by core-sheath PG provide a fascinating new strategy for tissue engineering. The hydroxyapatite-loaded fibrous sheath (PVA)

provides the environment and conditions required for biological activities in tissue engineering, while the core (PCL) acts as a mechanical support.^[51]

5.1.2. Drug Delivery

Polymer fibers, especially nanofibers, are one of the most promising carriers for drug delivery due to their unique high surface area-to-volume ratio, that allows high loading capacity and high encapsulation efficiency.^[110–112] Encapsulating hydrophobic drugs into hydrophilic polymer fibers by various means can help the issue of poor solubility of many drug molecules.^[113,114] The tunable characteristics of polymer fibers such as fiber diameter, morphology, and porosity help to modulate the drug release rate for specific therapy. Moreover, controlled release at the active site maximizes the effect of the drugs, achieving topical treatment and reducing drug dispersion.^[115,116] PG is one of the most potent strategies to create drug delivery systems due to its highly controllable processing parameters. Progesterone, an endogenous sex hormone that helps the development of the fetus and protects the endometrium during the female reproductive cycle, is widely used for the prevention of pre-term birth.^[117] Progesterone was mainly administered by oral or parenteral injection, but these methods have the problem of rapid metabolism and inactivation before taking effect or even causing some potential side effects.^[118] Fibrous patches for vaginal administration are a promising therapeutic strategy. Brako et al. and Cam et al. manufactured progesterone-loaded fibrous constructs with mucoadhesion by PG, which proved to be a successful method for vaginal administration for the treatment of pre-term birth.^[56,92–94] Oral antidiabetic agent-loaded fiber mats having different release kinetics (burst release or sustained release) produced by PG showed significant effects of accelerating wound healing and reducing inflammation in diabetes treatment.^[83,98] Sustained release delivery systems were reported to exhibit more effective results. Majd et al. produced PVP/PCL core-sheath fibers by core-sheath PG, which showed excellent encapsulation efficiency and controlled release of tetracycline hydrochloride.^[52] Core-sheath PG has immense potential in the encapsulation and controlled release of growth factors, drugs, and peptides in polymer fibers in a more precise manner.

5.1.3. Wound Dressing

Once the skin is structurally or functionally compromised, its function as the body's protective barrier will be hampered. The invasion of bacteria, fungi, viruses, etc. on the damaged site leads to slow healing, wound infection, and even life-threatening scenarios.^[119] Wound dressings are used to isolate the wound from pathogens, as well as provide a suitable physiological environment for wound healing.^[120] Compared with traditional textile dressings, which take effect only by isolation and secretion absorption, polymer fiber-based dressings show greater potential for wound healing.^[121–123] The small pore size and high porosity of fiber mats maintain good air permeability while isolating microorganisms. The 3D structure of fiber mats, which is similar to that of ECMs, and their proper mechanical strength facilitate cell growth, adhesion, and proliferation.^[124] The unique high

surface area-to-volume ratio of fine fibers is the significant carrier for antibacterial agents and drugs, which has been discussed above. Through the material selection and 3D structure design of the fiber products, polymer fiber-based dressings with excellent wound healing efficacy and good comfort were successfully fabricated by PG. With its inherent biocompatibility, bacterial cellulose (BC) is a fascinating candidate for wound dressings. The BC/PMMA binary fiber spun by PG not only overcame the difficulties of BC processing but also achieved the scalable production of natural polymer-based bandages.^[95] The BC/PMMA bandages incorporated with metal nanoparticles have been proven to show excellent cell viability and antibacterial properties, providing an attractive strategy for wound dressings.^[96] Ahmed et al. studied the antimicrobial properties and cytotoxicity of cinnamon-containing PCL bandages manufactured by PG, demonstrating the promising prospects of these natural active substance-based bandages.^[72,73]

PG can also be used in the applications of clinical imaging, diagnosis, therapy, etc. Mahalingam synthesized protein-coated polymer microbubbles using PG.^[64,65] The gold nanoparticles contained in these microbubbles have excellent chemical stability and biocompatibility, thus these have the potential of intracellular probes. In addition, the gold nanoparticles can be used to make quantum dots (Q dots) to be imaged in a bimodal way in both fluorescence and ultrasound, which is a complementary technology for ultrasound imaging. Lysozyme-coated PVA microbubbles were demonstrated to have good biosensing ability.

5.2. Filtration

With the development of industrialization, particulate pollutants in the air have become a significant environmental problem, threatening public health.^[125] Airborne aerosol particles containing bacteria and viruses are one of the main transmission routes of many emerging infectious diseases (EIDs), such as the SARS-CoV-2 that are prevalent worldwide.^[126,127] Besides this, water is also an important transmission medium of these tiny particulate pollutants.^[128] Separating these pollutants from air/water using filter materials is a crucial process in air/water purification. Fibrous materials with very small diameters have large surface area-to-volume ratios, high porosity, and small pore size, becoming effective filtration pads.^[5] Combining the features of forcespinning and solution blowing, PG is an efficient and facile method that allows additional jet stretching, obtaining nanofibers with average diameters of less than 500 nm.^[27,35,48,60,74,75,87,88,94] The unique surface effects of nanofibers effectively improve filtration efficiency. Filtration based on nanomaterials not only physically intercepts particles which are larger than the pore size through the sieve effect, but also captures extremely fine particles through the diffusion mechanism of the Brownian effect, or collisions with these particles.^[125,128–130] In addition, gas slip occurs on the nanofibers, thereby reducing air resistance.^[131] On the other hand, charged particles can be captured by electrostatic attraction with nanofibers.^[86,132] These nanofiber filters are promising for use in healthcare facilities, electronic component manufacturers, pharmaceuticals, personal protective equipment, and food where superior air purification is desired.^[128] Through spe-

cific solution property and processing parameter design, beaded fibers produced by PG can also be fashioned into viable filter media.^[44] This is due to the fact that the beaded structure increases the surface area of the filter and is beneficial to optimize the packing density. Moreover, the cavity structure caused by the beads further reduces the pressure drop by providing channels for airflow, which is an important criterion for evaluating filtration efficiency.^[86] Wrinkled and porous fibers with a very high surface area are also typical products of PG, which can improve the filtration performance of filters.^[53,59,84,126]

5.3. Energy Storage Applications

The development of new high-performance energy storage systems is a significant means to reduce the dependence on fossil fuels and promote the transition to clean energy. In addition to large specific surface area and unique surface effects, carbon nanofibers (CNFs) have considerable mechanical strength and excellent electrical conductivity, having great application potential in electrochemical energy storage.^[133] CNFs are generally used in rechargeable batteries and supercapacitors as active electrode materials, conductive additives, and metal/metal oxide-loaded substrates.^[134,135] On one hand, carbonaceous materials with high specific surface area and porous structure are conducive to storing ions. On the other hand, reversible surface or near-surface reactions of the loaded metals/metal oxides improve charge storage.^[136] Customized electrode materials with desired structures, sizes, morphologies, and compositions are of utmost importance for the development of superior energy storage systems. In addition, carbon nanotubes (CNTs) are also promising energy storage materials due to their higher electrical conductivity and larger surface area than CNFs.^[137,138] Polyacrylonitrile (PAN) is a material widely used to prepare CNFs due to its high carbon yield, high tensile strength, and relatively low price.^[139] The morphology of PAN fibers containing graphene oxide and graphene nanosheets prepared by PG highly depends on the processing parameters (rotational speed, working pressure, solution concentration, etc.) The mechanical properties and electrical conductivity of these fibers have been reported.^[54,85] Zhao et al. used PG to prepare PAN nanofibers loaded with CNTs, which has a 40% increase in specific capacitance and better reversibility, and is a promising material for rechargeable batteries.^[55]

Regarding commercial applications, the fiber materials market is vast in terms of market size and volume. In addition to the aforementioned uses (listed in Table 2), aerospace, automotive, and apparel manufacturing sectors have significant shares in the fiber market. The rising need for lightweight components due to the increasing demand for automotive and commercial aviation is propelling the fiber materials market, specifically for those with high-strength modulus and lightweight properties. In addition, polymer fibers are used in ultra-light clothing, fire-resistant and water-resistant textiles, and high-strength helmets, which also adds to the rising demand for fiber materials in the commercial sector.

6. The Future of Pressurized Gyration

Research related to PG has grown rapidly since its inception, which demonstrates its immense potential. At present, the ma-

terials used in PG are mainly synthetic polymers and organic solvents. Considering the pursuit of environmental friendliness and energy sustainability, spinning based on natural materials and green solvents will be a critical topic of PG in the future.^[140] Biopolymers, such as cellulose and alginate from plant sources, chitosan/chitin from animal sources, or polyhydroxyalkanoate from microbial sources, have received extensive attention due to their non-toxicity and inherent biocompatibility and biodegradability. According to a report by Transparency Market Research, the overall growth of biopolymer-based industries is forecast to expand at a staggering 14% between 2017 and 2025, and the market share of these industries will increase from USD 2.4 billion in 2016 to USD 7.8 billion by 2025.^[141] However, the manufacture of biopolymer fine fibers is not straightforward and has not yet been industrialized properly. The unique scalable and facile process of PG is expected to be a promising strategy for the mass production of biopolymer fibers.

Another prospect of PG is the preparation of hybrid fibers. Due to the features of producing fibers in multiple channels (orifices/nozzles), PG can be used to simultaneously process two or more materials from different channels to form a composite fiber mat. Hybrid fibers derive benefits from the individual fiber that exhibit a synergistic response, achieving the overall performance to exceed the sum of individual fiber performances. In addition, through the specific design of material types and proportions, hybrid fibers will achieve significant optimization in their mechanical properties.

Although the discussion on the significantly improved productivity of PG compared to other fiber manufacturing methods, such as electrospinning has been reported in previous work, at present the research is mainly carried out in the laboratory. Scale-up and fully-automated PG will be an important prerequisite for its industrialization. The critical concept of scale-up is related to the design of equipment matching the industrial scale and the introduction of a continuous feeding system. Automation requires electrical industrial robots with specific computer programming to realize the collection and packing of fiber products according to the set control system, which helps the reduction of the need for human work.

Acknowledgements

The authors would like to thank UKRI for supporting the development of pressurized gyration (Grants: EP/S016872/1, EP/N034228/1, EP/L023059/1). The authors appreciate many international (e.g., USA, China, Turkey, Italy) and UK collaborations, which created many opportunities and extra innovation to the work. Y.D. thanks the China Scholarship Council (CSC) for supporting her Ph.D. studies at University College London.

Conflict of Interest

The authors declare no conflict of interest.

Keywords

fibers, mass production, polymers, pressure, rotation

Received: February 2, 2023

Revised: March 23, 2023

Published online:

- [1] C. J. Luo, S. D. Stoyanov, E. Stride, E. Pelan, M. Edirisinghe, *Chem. Soc. Rev.* **2012**, *41*, 4708.
- [2] J. B. Donnet, R. C. Bansal, *Carbon fibers*, CRC Press, Boca Raton **1998**.
- [3] A. Barhoum, K. Pal, H. Rahier, H. Uludag, I. S. Kim, M. Bechelany, *Appl. Mater. Today* **2019**, *17*, 1.
- [4] X. H. Qin, S. Y. Wang, *J. Appl. Polym. Sci.* **2006**, *102*, 1285.
- [5] A. Podgorski, A. Balazy, L. Gradon, *Chem. Eng. Sci.* **2006**, *61*, 6804.
- [6] R. Gopal, S. Kaur, Z. W. Ma, C. Chan, S. Ramakrishna, T. Matsuura, *J. Membr. Sci.* **2006**, *281*, 581.
- [7] Q. H. Qiu, S. Y. Chen, Y. P. Li, Y. C. Yang, H. N. Zhang, Z. Z. Quan, X. H. Qin, R. W. Wang, J. Y. Yu, *Chem. Eng. J.* **2020**, *384*, 9.
- [8] M. Tebyetekerwa, Z. Xu, S. Y. Yang, S. Ramakrishna, *Adv. Fiber Mater.* **2020**, *2*, 161.
- [9] P. Serp, M. Corrias, P. Kalck, *Appl. Catal., A* **2003**, *253*, 337.
- [10] L. Persano, A. Camposo, D. Pisignano, *Prog. Polym. Sci.* **2015**, *43*, 48.
- [11] T. J. Sill, H. A. von Recum, *Biomaterials* **2008**, *29*, 1989.
- [12] Z. Ma, M. Kotaki, R. Inai, S. Ramakrishna, *Tissue Eng.* **2005**, *11*, 101.
- [13] E. Saino, M. L. Focarete, C. Gualandi, E. Emanuele, A. I. Cornaglia, M. Imbriani, L. Visai, *Biomacromolecules* **2011**, *12*, 1900.
- [14] A. Salam, T. Hassan, T. Jabri, S. Riaz, A. Khan, K. M. Iqbal, S. U. Khan, M. Wasim, M. R. Shah, M. Q. Khan, I. S. Kim, *Nanomaterials* **2021**, *11*, 13.
- [15] L. A. Alshabanah, M. Hagar, L. A. Al-Mutabagani, G. M. Abozaid, S. M. Abdallah, N. Shehata, H. Ahmed, A. H. Hassanin, *Polymers* **2021**, *13*, 14.
- [16] Y. Liu, J. Goebel, Y. Yin, *Chem. Soc. Rev.* **2013**, *42*, 2610.
- [17] H. Matsuyama, H. Okafuji, T. Maki, M. Teramoto, N. Kubota, *J. Membr. Sci.* **2003**, *223*, 119.
- [18] J. D. Hartgerink, E. Beniash, S. I. Stupp, *Science* **2001**, *294*, 1684.
- [19] Y. Dzenis, *Science* **2004**, *304*, 1917.
- [20] D. M. Dos Santos, D. S. Correa, E. S. Medeiros, J. E. Oliveira, L. H. Mattoso, *ACS Appl. Mater. Interfaces* **2020**, *12*, 45673.
- [21] Y. Wang, M. Zheng, H. Lu, S. Feng, G. Ji, J. Cao, *Nanoscale Res. Lett.* **2010**, *5*, 913.
- [22] W. Zhang, Z.-Y. Wu, H.-L. Jiang, S.-H. Yu, *J. Am. Chem. Soc.* **2014**, *136*, 14385.
- [23] L. F. Zhang, Y. L. Hsieh, *Eur. Polym. J.* **2009**, *45*, 47.
- [24] Q. Li, J. Zhang, Y. Wang, W. Qi, R. Su, Z. He, *Chemistry* **2018**, *24*, 18123.
- [25] N. Bhardwaj, S. C. Kundu, *Biotechnol. Adv.* **2010**, *28*, 325.
- [26] K. Sarkar, C. Gomez, S. Zambrano, M. Ramirez, E. de Hoyos, H. Vasquez, K. Lozano, *Mater. Today* **2010**, *13*, 12.
- [27] S. Mahalingam, M. Edirisinghe, *Macromol. Rapid Commun.* **2013**, *34*, 1134.
- [28] P. Mellado, H. A. McIlwee, M. R. Badrossamay, J. A. Goss, L. Mahadevan, K. K. Parker, *Appl. Phys. Lett.* **2011**, *99*, 203107.
- [29] H. Alenezi, M. E. Cam, M. Edirisinghe, *Appl. Phys. Rev.* **2019**, *6*, 041401.
- [30] R. T. Weitz, L. Harnau, S. Rauschenbach, M. Burghard, K. Kern, *Nano Lett.* **2008**, *8*, 1187.
- [31] H. Xu, H. Chen, X. Li, C. Liu, B. Yang, *J. Polym. Sci., Part B: Polym. Phys.* **2014**, *52*, 1547.
- [32] P. L. Heseltine, J. Ahmed, M. Edirisinghe, *Macromol. Mater. Eng.* **2018**, *303*, 1800218.
- [33] X. Zhang, Y. Lu, *Polym. Rev.* **2014**, *54*, 677.
- [34] A. Gañán-Calvo, *Phys. Rev. Lett.* **1998**, *80*, 285.
- [35] Y. Dai, J. Ahmed, A. Delbusso, M. Edirisinghe, *Macromol. Mater. Eng.* **2022**, *307*, 2200268.
- [36] E. S. Medeiros, G. M. Glenn, A. P. Klamczynski, W. J. Orts, L. H. C. Mattoso, *J. Appl. Polym. Sci.* **2009**, *113*, 2322.
- [37] R. Matharu, Z. Charani, L. Ciric, E. Illangakoon, M. Edirisinghe, *J. Appl. Polym. Sci.* **2018**, *135*, 46368.

- [38] B. T. Raimi-Abraham, S. Mahalingam, M. Edirisinghe, D. Q. M. Craig, *Mater. Sci. Eng., C* **2014**, *39*, 168.
- [39] M. Gultekinoglu, Ş. Öztürk, B. Chen, M. Edirisinghe, K. Ulubayram, *Eur. Polym. J.* **2019**, *121*, 109297.
- [40] S. Mahalingam, S. Homer-Vanniasinkam, M. Edirisinghe, *Mater. Des.* **2019**, *178*, 107846.
- [41] S. Mahalingam, S. Huo, S. Homer-Vanniasinkam, M. Edirisinghe, *Polymers* **2020**, *12*, 1709.
- [42] P. Mehta, M. Rasekh, M. Patel, E. Onaiwu, K. Nazari, I. Kucuk, P. B. Wilson, M. S. Arshad, Z. Ahmad, M. W. Chang, *Adv. Drug Delivery Rev.* **2021**, *175*, 113823.
- [43] Y. Ide, J. L. White, *J. Appl. Polym. Sci.* **1976**, *20*, 2511.
- [44] X. Hong, M. Edirisinghe, S. Mahalingam, *Mater. Sci. Eng., C* **2016**, *69*, 1373.
- [45] X. Hong, S. Mahalingam, M. Edirisinghe, *Macromol. Mater. Eng.* **2017**, *302*, 1600564.
- [46] Z. Xu, S. Mahalingam, P. Basnett, B. Raimi-Abraham, I. Roy, D. Craig, M. Edirisinghe, *Macromol. Mater. Eng.* **2016**, *301*, 922.
- [47] X. Hong, A. Harker, M. Edirisinghe, *ACS Omega* **2018**, *3*, 5470.
- [48] X. Hong, A. Harker, M. Edirisinghe, *Proc. R. Soc. A* **2019**, *475*, 20190008.
- [49] H. Alenezi, M. E. Cam, M. Edirisinghe, *Appl. Phys. Rev.* **2021**, *8*, 041412.
- [50] S. Mahalingam, R. Matharu, S. Homer-Vanniasinkam, M. Edirisinghe, *Appl. Phys. Rev.* **2020**, *7*, 041302.
- [51] S. Mahalingam, C. Bayram, M. Gultekinoglu, K. Ulubayram, S. Homer-Vanniasinkam, M. Edirisinghe, *Macromol. Biosci.* **2021**, *21*, 2100177.
- [52] H. Majd, A. Harker, M. Edirisinghe, M. Parhizkar, *J. Drug Delivery Sci. Technol.* **2022**, *72*, 103359.
- [53] U. E. Illangakoon, S. Mahalingam, R. K. Matharu, M. Edirisinghe, *Polymers* **2017**, *9*, 508.
- [54] A. Amir, H. Porwal, S. Mahalingam, X. Wu, T. Wu, B. Chen, T. A. Tabish, M. Edirisinghe, *Compos. Sci. Technol.* **2020**, *197*, 108214.
- [55] H. Zhao, X. Wu, J. Liu, Z. Huang, Y.-g. Liu, M. Fang, X. Min, *J. Mater. Res.* **2018**, *33*, 4251.
- [56] M. E. Cam, A. N. Hazar-Yavuz, S. Cesur, O. Ozkan, H. Alenezi, H. T. Sasmazel, M. S. Eroglu, F. Brako, J. Ahmed, L. Kabasakal, *Int. J. Pharm.* **2020**, *588*, 119782.
- [57] P. L. Heseltine, J. Hosken, C. Agboh, D. Farrar, S. Homer-Vanniasinkam, M. Edirisinghe, *Macromol. Mater. Eng.* **2019**, *304*, 1800577.
- [58] P. L. Heseltine, C. Bayram, M. Gultekinoglu, S. Homer-Vanniasinkam, K. Ulubayram, M. Edirisinghe, *ACS Biomater. Sci. Eng.* **2022**, *8*, 1290.
- [59] P. Basnett, R. K. Matharu, C. S. Taylor, U. Illangakoon, J. I. Dawson, J. M. Kanczler, M. Behbehani, E. Humphrey, Q. Majid, B. Lukasiewicz, *ACS Appl. Mater. Interfaces* **2021**, *13*, 32624.
- [60] S. Mahalingam, G. Ren, M. Edirisinghe, *Carbohydr. Polym.* **2014**, *114*, 279.
- [61] B. O. Boskovic, V. B. Golovko, M. Cantoro, B. Kleinsorge, A. T. H. Chuang, C. Ducati, S. Hofmann, J. Robertson, B. F. G. Johnson, *Carbon* **2005**, *43*, 2643.
- [62] C. Wang, R. Zaouk, M. Madou, *Carbon* **2006**, *44*, 3073.
- [63] S. Mahalingam, G. Pierin, P. Colombo, M. Edirisinghe, *Ceram. Int.* **2015**, *41*, 6067.
- [64] S. Mahalingam, Z. Xu, M. Edirisinghe, *Langmuir* **2015**, *31*, 9771.
- [65] S. Mahalingam, B. T. Raimi-Abraham, D. Q. Craig, M. Edirisinghe, *Langmuir* **2015**, *31*, 659.
- [66] J. R. Lindner, *Nat. Rev. Drug Discovery* **2004**, *3*, 527.
- [67] S. Cesur, M. E. Cam, F. S. Sayin, S. Su, A. Harker, M. Edirisinghe, O. Gunduz, *Langmuir* **2022**, *38*, 5040.
- [68] P. Dijkmans, L. Juffermans, R. Musters, A. van Wamel, F. Ten Cate, W. van Gilst, C. Visser, N. de Jong, O. Kamp, *Eur. J. Echocardiogr.* **2004**, *5*, 245.
- [69] J. M. Tsutsui, F. Xie, R. T. Porter, *Cardiovasc. Ultrasound* **2004**, *2*, 23.
- [70] K. Kundu, A. Afshar, D. R. Katti, M. Edirisinghe, K. S. Katti, *Compos. Sci. Technol.* **2021**, *202*, 108598.
- [71] M. O. Aydogdu, E. Altun, J. Ahmed, O. Gunduz, M. Edirisinghe, *Polymers* **2019**, *11*, 1148.
- [72] J. Ahmed, E. Altun, M. O. Aydogdu, O. Gunduz, L. Kerai, G. Ren, M. Edirisinghe, *Int. Wound J.* **2019**, *16*, 730.
- [73] J. Ahmed, M. Gultekinoglu, C. Bayram, D. Kart, K. Ulubayram, M. Edirisinghe, *MedComm* **2021**, *2*, 236.
- [74] S. Zhang, B. T. Karaca, S. K. VanOosten, E. Yuca, S. Mahalingam, M. Edirisinghe, C. Tamerler, *Macromol. Rapid Commun.* **2015**, *36*, 1322.
- [75] U. E. Illangakoon, S. Mahalingam, P. Colombo, M. Edirisinghe, *Surf. Innovations* **2016**, *4*, 167.
- [76] M. Karimpoor, E. Illangakoon, A. G. Reid, S. Claudiani, M. Edirisinghe, J. S. Khorashad, *Br. J. Haematol.* **2018**, *182*, 924.
- [77] R. K. Matharu, T. A. Tabish, T. Trakoolwilaiwan, J. Mansfield, J. Moger, T. Wu, C. Lourenço, B. Chen, L. Ciric, I. P. Parkin, *J. Colloid Interface Sci.* **2020**, *571*, 239.
- [78] R. K. Matharu, L. Ciric, G. Ren, M. Edirisinghe, *Nanomaterials* **2020**, *10*, 1017.
- [79] U. E. Illangakoon, S. Mahalingam, K. Wang, Y. K. Cheong, E. Canales, G. Ren, E. Cloutman-Green, M. Edirisinghe, L. Ciric, *Mater. Sci. Eng., C* **2017**, *74*, 315.
- [80] R. K. Matharu, H. Porwal, L. Ciric, M. Edirisinghe, *Interface Focus* **2018**, *8*, 20170058.
- [81] J. Ahmed, R. K. Matharu, T. Shams, U. E. Illangakoon, M. Edirisinghe, *Macromol. Mater. Eng.* **2018**, *303*, 1700577.
- [82] B. T. Raimi-Abraham, S. Mahalingam, P. J. Davies, M. Edirisinghe, D. Q. Craig, *Mol. Pharmaceutics* **2015**, *12*, 3851.
- [83] M. E. Cam, S. Yildiz, H. Alenezi, S. Cesur, G. S. Ozcan, G. Erdemir, U. Edirisinghe, D. Akakin, D. S. Kuruca, L. Kabasakal, *J. R. Soc., Interface* **2020**, *17*, 20190712.
- [84] S. Mahalingam, X. Wu, M. Edirisinghe, *Mater. Des.* **2017**, *134*, 259.
- [85] X. Wu, S. Mahalingam, A. Amir, H. Porwal, M. J. Reece, V. Naglieri, P. Colombo, M. Edirisinghe, *ACS Omega* **2016**, *1*, 202.
- [86] R. Huang, Y. Dai, J. Ahmed, M. Edirisinghe, *Polymers* **2022**, *14*, 4498.
- [87] S. Mahalingam, B. T. Raimi-Abraham, D. Q. Craig, M. Edirisinghe, *Chem. Eng. J.* **2015**, *280*, 344.
- [88] Z. Xu, S. Mahalingam, J. Rohn, G. Ren, M. Edirisinghe, *Mater. Sci. Eng., C* **2015**, *56*, 195.
- [89] A. Amir, S. Mahalingam, X. Wu, H. Porwal, P. Colombo, M. J. Reece, M. Edirisinghe, *Compos. Sci. Technol.* **2016**, *129*, 173.
- [90] X. Su, S. Mahalingam, M. Edirisinghe, B. Chen, *ACS Appl. Mater. Interfaces* **2017**, *9*, 22223.
- [91] A. Kelly, J. Ahmed, M. Edirisinghe, *Macromol. Mater. Eng.* **2022**, *307*, 2100891.
- [92] F. Brako, R. Thorogate, S. Mahalingam, B. Raimi-Abraham, D. Q. Craig, M. Edirisinghe, *ACS Appl. Mater. Interfaces* **2018**, *10*, 13381.
- [93] F. Brako, B. T. Raimi-Abraham, S. Mahalingam, D. Q. Craig, M. Edirisinghe, *Int. J. Pharm.* **2018**, *540*, 31.
- [94] F. Brako, B. Raimi-Abraham, S. Mahalingam, D. Q. Craig, M. Edirisinghe, *Eur. Polym. J.* **2015**, *70*, 186.
- [95] E. Altun, M. O. Aydogdu, F. Koc, M. Crabbe-Mann, F. Brako, R. Kaur-Matharu, G. Ozen, S. E. Kuruca, U. Edirisinghe, O. Gunduz, *Macromol. Mater. Eng.* **2018**, *303*, 1700607.
- [96] E. Altun, M. O. Aydogdu, M. Crabbe-Mann, J. Ahmed, F. Brako, B. Karademir, B. Aksu, M. Sennaroglu, M. S. Eroglu, G. Ren, *Macromol. Mater. Eng.* **2019**, *304*, 1800537.
- [97] X. Wu, S. Mahalingam, S. K. VanOosten, C. Wisdom, C. Tamerler, M. Edirisinghe, *Macromol. Biosci.* **2017**, *17*, 1600270.
- [98] M. E. Cam, B. Ertas, H. Alenezi, A. N. Hazar-Yavuz, S. Cesur, G. S. Ozcan, C. Ektok, E. Guler, C. Katsakouli, Z. Demirbas, *Mater. Sci. Eng., C* **2021**, *119*, 111586.

- [99] R. M. Rowell, in *Properties and Performance of Natural-Fibre Composites*, (Ed.: K. L. Pickering), Woodhead Publishing, Cambridge **2008**, p. 3.
- [100] S. Gungordu Er, A. Kelly, S. B. W. Jayasuriya, M. Edirisinghe, *Biomed. Mater. Diagn. Devices* **2022**.
- [101] S. Nemati, S. J. Kim, Y. M. Shin, H. Shin, *Nano Convergence* **2019**, *6*, 36.
- [102] R. L. Dahlin, F. K. Kasper, A. G. Mikos, *Tissue Eng., Part B* **2011**, *17*, 349.
- [103] J. Fang, H. Niu, T. Lin, X. Wang, *Chin. Sci. Bull.* **2008**, *53*, 2265.
- [104] Q. P. Pham, U. Sharma, A. G. Mikos, *Tissue Eng.* **2006**, *12*, 1197.
- [105] M. Ottosson, A. Jakobsson, F. Johansson, *PLoS One* **2017**, *12*, e0169419.
- [106] B. M. Baker, A. O. Gee, R. B. Metter, A. S. Nathan, R. A. Marklein, J. A. Burdick, R. L. Mauck, *Biomaterials* **2008**, *29*, 2348.
- [107] S. Zhong, W. E. Teo, X. Zhu, R. W. Beuerman, S. Ramakrishna, L. Y. L. Yung, *J. Biomed. Mater. Res., Part A* **2006**, *79A*, 456.
- [108] J. Nam, Y. Huang, S. Agarwal, J. Lannutti, *Tissue Eng.* **2007**, *13*, 2249.
- [109] S. Soliman, S. Sant, J. W. Nichol, M. Khabiry, E. Traversa, A. Khademhosseini, *J. Biomed. Mater. Res., Part A* **2011**, *96A*, 566.
- [110] X. Hu, S. Liu, G. Zhou, Y. Huang, Z. Xie, X. Jing, *J. Controlled Release* **2014**, *185*, 12.
- [111] B. Wang, Y. Wang, T. Yin, Q. Yu, *Chem. Eng. Commun.* **2010**, *197*, 1315.
- [112] E. R. Kenawy, F. I. Abdel-Hay, M. H. El-Newehy, G. E. Wnek, in *Nanomaterials: Risks and Benefits*, Springer, Dordrecht **2009**, p. 247.
- [113] S. Kalepu, V. Nekkanti, *Acta Pharm. Sin. B* **2015**, *5*, 442.
- [114] F. Ignatious, L. Sun, C. P. Lee, J. Baldoni, *Pharm. Res.* **2010**, *27*, 576.
- [115] A. Luraghi, F. Peri, L. Moroni, *J. Controlled Release* **2021**, *334*, 463.
- [116] T. J. Sill, H. A. von Recum, *Biomaterials* **2008**, *29*, 1989.
- [117] R. Romero, L. Yeo, P. Chaemsaitong, T. Chaiworapongsa, S. S. Hassan, *Semin. Fetal Neonat. Med.* **2014**, *19*, 15.
- [118] H. C. Zierden, R. L. Shapiro, K. DeLong, D. M. Carter, L. M. Ensign, *Adv. Drug Delivery Rev.* **2021**, *174*, 190.
- [119] G. Broughton II, J. E. Janis, C. E. Attinger, *Plast. Reconstr. Surg.* **2006**, *117*, 1e-S.
- [120] S. Dhivya, V. V. Padma, E. Santhini, *BioMedicine* **2015**, *5*, 22.
- [121] F. Wang, S. Hu, Q. Jia, L. Zhang, *J. Nanomater.* **2020**, *2020*, 8719859.
- [122] Y. F. Goh, I. Shakir, R. Hussain, *J. Mater. Sci.* **2013**, *48*, 3027.
- [123] S. Schreml, R.-M. Szeimies, L. Prantl, M. Landthaler, P. Babilas, *J. Am. Acad. Dermatol.* **2010**, *63*, 866.
- [124] Y. Liu, T. Li, Y. Han, F. Li, Y. Liu, *Curr. Opin. Biomed. Eng.* **2021**, *17*, 100247.
- [125] V. V. Kadam, L. Wang, R. Padhye, *J. Ind. Text.* **2018**, *47*, 2253.
- [126] T. Lu, J. Cui, Q. Qu, Y. Wang, J. Zhang, R. Xiong, W. Ma, C. Huang, *ACS Appl. Mater. Interfaces* **2021**, *13*, 23293.
- [127] K. Azuma, U. Yanagi, N. Kagi, H. Kim, M. Ogata, M. Hayashi, *Environ. Health Prev. Med.* **2020**, *25*, 66.
- [128] R. S. Barhate, S. Ramakrishna, *J. Membr. Sci.* **2007**, *296*, 1.
- [129] X. Qin, S. Subianto, in *Electrospun Nanofibers*, (Ed.: M. Afshari), Woodhead Publishing, Cambridge **2017**, p. 449.
- [130] J. Wang, S. C. Kim, D. Y. H. Pui, *J. Aerosol Sci.* **2008**, *39*, 323.
- [131] Q. Zhang, J. Welch, H. Park, C. Y. Wu, W. Sigmund, J. C. M. Marijnissen, *J. Aerosol Sci.* **2010**, *41*, 230.
- [132] C. D. Zangmeister, J. G. Radney, E. P. Vicenzi, J. L. Weaver, *ACS Nano* **2020**, *14*, 9188.
- [133] L. Ji, Z. Lin, A. J. Medford, X. Zhang, *Carbon* **2009**, *47*, 3346.
- [134] B. Zhang, F. Kang, J. M. Tarascon, J. K. Kim, *Prog. Mater. Sci.* **2016**, *76*, 319.
- [135] Q. Liu, J. Zhu, L. Zhang, Y. Qiu, *Renewable Sustainable Energy Rev.* **2018**, *81*, 1825.
- [136] X. Li, Y. Chen, H. Huang, Y.-W. Mai, L. Zhou, *Energy Storage Mater.* **2016**, *5*, 58.
- [137] L. Sun, X. Wang, Y. Wang, Q. Zhang, *Carbon* **2017**, *122*, 462.
- [138] L. Wen, F. Li, H.-M. Cheng, *Adv. Mater.* **2016**, *28*, 4306.
- [139] D. Jang, M. E. Lee, J. Choi, S. Y. Cho, S. Lee, *Carbon* **2022**, *186*, 644.
- [140] M. Amarakoon, H. Alenezi, S. Homer-Vanniasinkam, M. Edirisinghe, *Macromol. Mater. Eng.* **2022**, *307*, 2200356.
- [141] A. Kakoria, S. Sinha-Ray, *Fibers* **2018**, *6*, 45.



Yanqi Dai is a Ph.D. student in the Department of Mechanical Engineering at University College London. She received her B.Sc. in materials science and engineering from Xiamen University, China, followed by an M.Sc. in biomaterials and tissue engineering with distinction from University College London in 2020. Her current research focuses on the design of novel processes and devices for fiber manufacturing and the preparation of sustainable biopolymer fibers.



Jubair Ahmed is a postdoctoral researcher at University College London where he completed his Ph.D. in 2022. His background is in biochemistry as well as in biomaterials and tissue engineering. His current research focuses on the sustainable production of polymeric fibers for healthcare-related biomedical applications. He has published 21 papers, and has an h-index of 10 with over 480 citations. He has had collaborations with many groups spanning multiple countries including the USA, Turkey, and India. Jubair has a particular interest in technologies encapsulating biotechnology, information processing, and multimedia relating to expanding public awareness of science and technology.



Mohan Edirisinghe is Bonfield Chair of Biomaterials in UCL Mechanical Engineering. He has published over 600 journal papers. His research on materials and manufacturing for healthcare has won numerous grants and prizes, including recently, the UK Royal Academy of Engineering Prize for Excellence in Materials Engineering and the Premier UK IOM3 Chapman Medal for Distinguished Research in Biomedical Materials. In the Queen's New Year National Honors 2021, he was appointed OBE for his services to biomedical engineering. His most recent work on innovative manufacturing of polymer fibers using pressurized gyration invented in 2013 has won 17 journal cover-papers to date.